Letter

Exploiting Confinement Effects to Tune Selectivity in Cyclooctane Metathesis

Eva Pump, Zhen Cao, Manoja K Samantaray, Anissa Bendjeriou-Sedjerari, Luigi Cavallo, and Jean-Marie Basset

ACS Catal., **Just Accepted Manuscript** • DOI: 10.1021/acscatal.7b01249 • Publication Date (Web): 24 Aug 2017

Exploiting Confinement Effects to Tune Selectivity in Cyclooctane Metathesis

Eva Pump, Zhen Cao, Manoja K. Samantaray, Anissa Bendjeriou-Sedjerari,* Luigi Cavallo,* and Jean-Marie Basset*.

King Abdullah University of Science and Technology (KAUST), KAUST Catalysis Center (KCC), Thuwal, 23955-6900 (Saudi Arabia).

alkane metathesis • confinement effect • DFT • mesoporous catalyst • surface organometallic chemistry (SOMC).

ABSTRACT: The mechanism of cyclooctane metathesis using confinement effect strategies in mesoporous silica nanoparticles (MSNs) is discussed by catalytic experiments and density functional theory (DFT) calculations. WMe_6 was immobilized inside the pores of a series of MSNs having the same structure but different pore diameters (60, 30 and 25 Å). Experiments in cyclooctane metathesis suggest that confinement effects observed in smaller pores (30 and 25 Å) improve selectivity towards the dimeric cyclohexadecane. In contrast, in larger pores (60 Å) a broad product distribution dominated by ring contracted cycloalkanes was found. The catalytic cycle and potential side reactions occurring at [(≡SiO-)WMe_5] were examined with DFT calculations. Analysis of the geometries for the key reaction intermediates allowed to rationalize the impact of a confined environment on the enhanced selectivity towards the dimeric product in smaller pores, while in large pores the ring contracted products are favored.

Confinement effects[1-4] have been invoked in heterogeneous catalysis to improve the selectivity (e.g. asymmetric synthesis,[4-5] hydrocarbon cracking,[6-8] methanol to olefin conversion[9]) by using nanostructured catalysts. A confinement effect has also been described in olefin metathesis of cyclic olefins using mesoporous supported catalysts:[10] In cyclooctene metathesis, depending on the pore sizes of the supported catalysts, more polymeric (large pores) or more cyclic, oligomeric (dimers, trimers and tetramers) products were found. Alkane metathesis,[11-13] which includes an olefin metathesis step in its mechanism,[11-14] seems to be another attractive reaction to improve selectivity by exploiting confinement effects. The main difference between both reactions (olefin and alkane metathesis) is the dehydrogenation/hydrogenation steps which occurs in alkane metathesis before and after the olefin metathesis step and converts alkane into alkene and, after olefin metathesis, the new-formed alkene back into alkanes.[11] A broad product distribution is typically found in alkane metathesis using a multifunctional surface organometallic chemistry (SOMC) catalysts suggesting that, besides the abovementioned steps, another side reaction occurs, namely double bond migration (DBM)[14] which led us to call metathesis of alkanes "*iso*-metathesis of alkanes". Its competition with ring opening metathesis (ROM) and ring closing metathesis (RCM) leads to the formation of higher and lower analogues of the starting alkane.[15-16] Previously, cyclooctane (cC_8) metathesis, using the surface organometallic fragment (SOMF) [(≡SiO-)WMe_5] **A**, immobilized on silica nanoparticles (**Ao**) was shown to give mainly ring contracted products as cyclopentane, cyclohexane and cycloheptane (cC_5, cC_6, cC_7) and dimeric cyclohexadecane (cC_{16}) as a secondary product.[15] By applying the confinement strategy for the same reaction, an improved selectivity towards the dimer cC_{16} was obtained using small pore sizes, while mainly ring contracted products (cC_5-cC_7) were detected using larger pore sizes. This unexpected results is explained by theoretical modeling demonstrating that the effective volume and the shape (Sterimol parameter)[17-18] of the main intermediates (metallacycles) play a critical role in orienting the reaction toward dimerization (ROM/RCM) or ring contraction (ROM/DBM/RCM).

Typically, materials are prepared through the SOMC[19-20] approach allowing well-defined catalyst supported on silica,[21-23] alumina[24] or silica-alumina.[16, 25] To be in line with the concept of "Catalysis by Design",[26] several physical parameters of the support need to be considered, as pore size and structure, aggregation properties and particle size. Herein, we focus on tuning the pore size of the mesoporous silica support (SBA15 and MCM41 having the same hexagonal structure, but different pore diameters [d_{pore} = 60 Å (**1**), 30 Å (**2**) and 25 Å (**3**)]).[27-29] In any of these systems we found a similar, very broad distribution of particle size (between 200-1000 nm). Subsequently, WMe_6 was immobilized on **1**, **2** and **3** to form [(≡SiO-)WMe_5] **A** inside the mesopores.[22] The mesoporous support was treated at 500°C under high vacuum (10^{-5} mbar) which is the maximum temperature which can be applied to prevent MCM-41 from collapsing[30] and the minimum temperature to obtain

isolated silanols (≡SiOH)[31]. It is noteworthy that the thermal treatment of mesoporous material induce the disappearance of the micropores which do not affect the catalytic results (Table S1, ESI†). The successful grafting of WMe_6 inside the mesopores forming **A1**, **A2** and **A3** was shown previously[22] by N_2 sorption, TEM (Figure S1 and S2, ESI†) and dynamic nuclear polarization surface enhanced NMR spectroscopy (DNP-SENS). Catalysts **A1**, **A2** and **A3** were tested in cC_8 metathesis and compared with results obtained with catalyst **A0**[15] (Figure 1). Promising trends were obtained regarding the selectivity towards the desired product cC_{16}: When considering all formed products, the selectivity for cC_{16} increases with decreasing d_{pore} of MSNs.

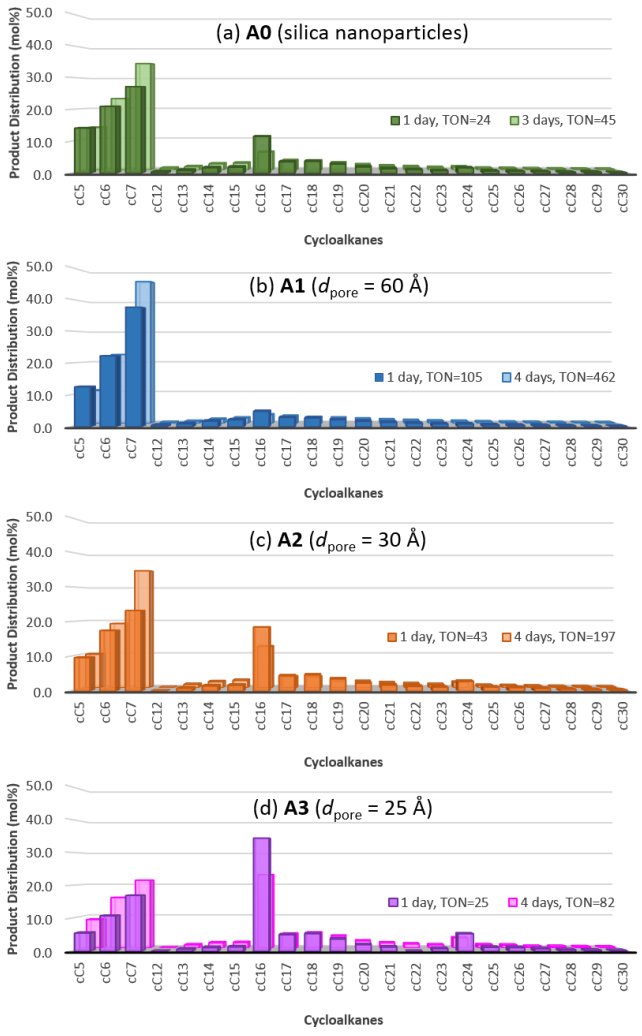

Figure 1. Product distributions of cC_8 (3.7 mmol (**A0**) and 7.4 mmol (**A1**, **A2**, **A3**)) metathesis at 150°C (batch reactor) after 1 (front) and 3-4 days (back) catalyzed by **A** bearing different supports. (a) **A0**: silica nanoparticles, $d_{particle}$ = 120 Å, [W]: 6.5 µmol;[15, 32] (b) **A1**: SBA15, d_{pore} = 60 Å, [W]: 12.4 µmol; (c) **A2**: MCM41, d_{pore} = 30 Å, [W]: 14.8 µmol; (d) **A3**: MCM41, d_{pore} = 25 Å, [W]: 8.7 µmol.

After one day, **A1** (with the largest pore diameter) produces only 5% of cC_{16}, while **A2** yields 18% and **A3** even 34% of cC_{16}. Contrary, the sum of the ring contracted products [$\Sigma(cC_5, cC_6, cC_7)$] decreases in the same order from 63%, to 50% and 34%, respectively. After four days, the selectivity for cC_{16} decreases in all cases by up to 40% ending up with 3% (**A1**), 12% (**A2**) and 23% (**A3**) of cC_{16}. Nevertheless, the selectivity for the dimer cC_{16} is maintained using **A3** (23%), and was found to be the main product after 4 days. It is noteworthy to mention that catalyst **A0** presents a better selectivity towards cC_{16} compared to **A1** (12% vs. 5%), but a decreased selectivity as **A2** and **A3** (18%, 34%, respectively, vs. 12%).The most suitable explanation for this result is the aggregation of silica nanoparticles in non-polar solvent[33] (as cC_8) which probably creates interparticular spaces between the nanoparticles evoking a similar confinement effect for **A0** as found for **A2** and **A3**, however less pronounced (Figure S3, ESI†). The fact that selectivity towards the dimer cC_{16} can be improved with **A0** when the reaction is not stirred further supports this indication.[15] It is known that the confinement strategy is affected by (i) the low accessibility of the active sites and (ii) a hindered diffusion of the substrate or product inside the mesopores.[2] Hence, it is not surprising that also the TONs of **A1**, **A2** and **A3** (after 1 day) drop from 105 to 42 and 25, respectively, when reducing the mesoporous diameter from 60 (**A1**) to 30 (**A2**) and 25 Å (**A3**).

The most crucial steps of the transformation of cC_8 catalyzed by **A** are the dehydrogenation (I), olefin metathesis (II) and hydrogenation (III) and were explained in previous work.[12, 15] It was reported that thermal activation of **A**, involves an intramolecular CH-activation by releasing two methane molecules, forming [(≡SiO-)W(≡CH)Me_2] **B**.[21] DFT calculations of the activation mechanism (Figure S7-S9, ESI†) indicate a CH-activation of cyclooctane with the W(≡CH) triple bond (Figure 2a) forming [(≡SiO-)W(=CH_2)$(Me)_2$(cC_8)] **C**. A subsequent β-H elimination and decoordination of the formed olefin leads to the active site [(≡SiO-)W(=CH_2)$(Me)_2$(H)] **D**.[34] Other activation pathways (including the tautomer of **B**, [(≡SiO-)W(=CH_2)$_2$Me] **B$_2$**)[35] are excluded as the energy barriers for the rate determining step (CH-bond activation) clearly exceed the one of the proposed activation mechanism by at least around 10 kcal/mol (Figure S8, ESI†).

The initial steps of cC_8 metathesis (common for cC_7-, cC_8-, cC_9- and cC_{16}-pathways) were reported previously.[15] For the sake of readability, we briefly recapitulate the main conclusions for cC_8 (Figure 2b). (i) CH-activation with cC_8 and the active species **D** releases hydrogen and forms **C**. (ii) β-H elimination of the cyclooctyl-ligand leads to the coordination intermediate **E**. (iii) The coordinated cyclooctene reacts with the [W]=CH_2 moiety forming metallacycle **F**. (iv) A subsequent opening of the metallacycle leads to the coordination intermediate **G**. (v) Decoordination of the double bond leads to the open [(≡SiO-)W(=nonenylidene)$_2$Me] intermediate **o**. (vi) A subsequent CH-activation with another cC_8 leads to **1** (Figure S9, ESI), which is the actual starting point of this theoretical study. The dimer cC_{16} is generated from **1** through β-H-elimination and a successive ROM and RCM of the internal and terminal double bond (**1-9**, Figure 2c). The formation of ring contracted products (and other products containing a carbon number other than a multiple of 8) is explained by

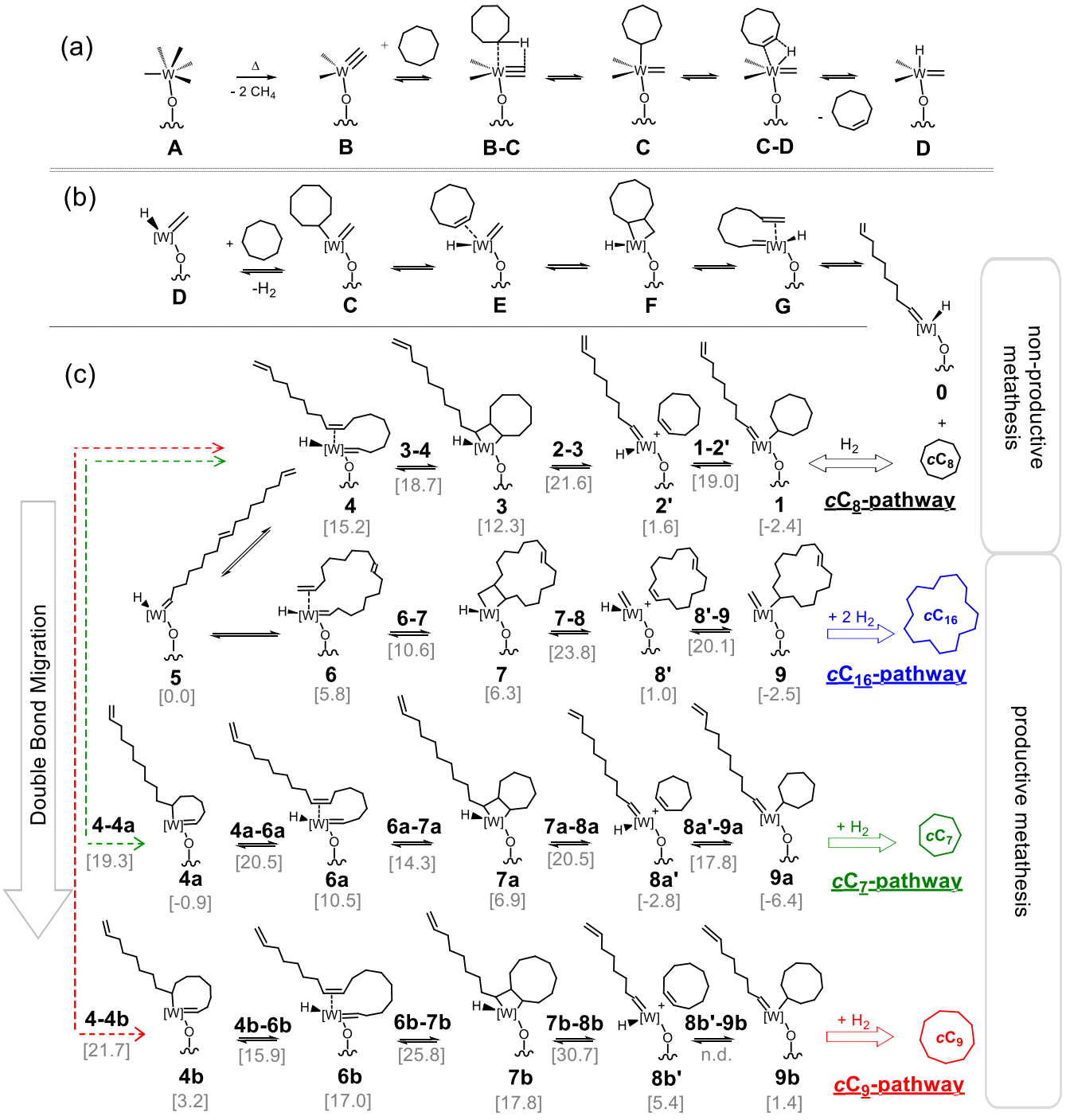

Figure 2. (a) Formation of active species [(≡SiO-)W(=CH$_2$)Me$_2$H] **D** from *pre*-catalyst [(≡SiO-)WMe$_5$] **A** through intermediates [(≡SiO-)W(≡CH)Me$_2$] **B** (experimentally observed) and [(≡SiO-)W(=CH)(*c*C$_8$)Me$_2$] **C** and concomitant transition states **B-C** and **C-D**. (b) Initial steps of *c*C$_8$ metathesis, illustrating the formation of **1** starting from the active site [(≡SiO-)W(=CH$_2$)Me$_2$H] **D** through CH-activation by σ-bond metathesis of *c*C$_8$ and ring opening metathesis (ROM) through intermediates **C**, **E**, **F**, **G**, and **H**. (c) Ring-opening-ring closing metathesis (ROM-RCM) for *c*C$_8$ (**1-5**) metathesis leading to *c*C$_{16}$ (**5-9**) and to *c*C$_7$ (**4-9a**) and *c*C$_9$ (**4-9b**) through a preceding double bond migration. The bold numbers indicate the labeling of the intermediates and transition states, the [grey] numbers in parenthesis represent the free energies (ΔG) in kcal/mol, which were determined by DFT calculations (M06/TZVP//BP86/SVP, pcm=cyclohexane, P=1354 atm).

a concurring DBM in intermediate **4** (towards **4a** or **4b**, Figure 2c). The occurrence of a chain walking process is already known in alkane metathesis[14] and proceeds via the simple insertion of the double bond into the W-H bond followed by β-H elimination. The mechanism of ROM-RCM (*c*C$_8$-pathway, *c*C$_{16}$-pathway) and ROM-DBM-RCM (*c*C$_7$-pathway, *c*C$_9$-pathway) are summarized in Figure 2c and Figure S11, S12 and S13, in ESI†. The final alkane will be generated through stepwise hydrogenation of the new olefin (costs approximately 15 kcal/mol), which can be achieved with only a small steady state concentration of H$_2$[34] (Figure S9, ESI†). Herein, we focus on the competition

between olefin metathesis and DBM steps. The key steps of the respective pathways are discussed using intermediate **5** as reference structure at 0.0 kcal/mol. To rationalize the formation of cC_{16}, the respective reaction pathway (cC_{16}-pathway in Figure 2c and Figure S11, ESI†) was investigated. The most important observations are highlighted in the following. (i) Intramolecular coordination (back biting) of the terminal double bond (leading from **5** to **6**) is more favorable than coordination of the internal double bond (from **5** to **4**) by roughly 10 kcal/mol. (ii) Comparing the opening step of the metallacycles **3** (leading to **2**) and **7** (leading to **8**), we found that the disubstituted tungstacyclobutane complex **7** is more stable towards the loss of the olefin than the trisubstituted tungstacyclobutane complex **3**, presumably for steric reasons (the metallacycle of **7** is disubstituted whereas the metallacycle **3** is trisubstituted and we found this difference to be crucial in the stereochemistry of olefin metathesis).[36-37] This step (23.8 kcal/mol) can be described as the rate determining step of ROM/RCM reaction (excluding CH-bond activation in the activation and initiation steps, Figure S9, ESI†). (iii) The olefin is released from the rather unstable coordination intermediate **8** (21.0 kcal/mol) to form intermediate **8'** (1.0 kcal/mol). From there, the cC_{16} double bond inserts into the [W]-hydride (**8'-9**) forming intermediate **9**, which costs 20.1 kcal/mol. The thermodynamically more stable, saturated dimer cC_{16} is formed by two consecutive hydrogenolysis steps (Figure S9, ESI†). Side products (other than cC_{16}) are formed because, under the applied reaction conditions, DBM occurs (**4-9a**, **4-9b** in Figure 2c, Figure S12, ESI†) requiring a maximum barrier of around 22 kcal/mol. Starting from **4**, with a C^8=C^9 double bond coordinated to the metal, two new coordination intermediates can be formed depending on the direction of the C=C insertion into the W-H bond: a 7-membered coordination intermediate **6a** presenting a C^7=C^8 double bond (cC_7-pathway in Figure 2c) and a 9-membered coordination intermediate **6b**, presenting a C^9=C^{10} double bond (cC_9-pathway in Figure 2c). Having obtained four relevant coordination intermediates, we describe the peculiarities of RCM for cC_7-, cC_9-, and cC_{16}-productive pathways (**6a**, **6b** and **6**, respectively), together with the non-productive cC_8-pathway regenerating the starting cC_8 from **4** (degenerate alkane metathesis). These pathways are compared in Figure 2c (and Figure S13, ESI†) using again intermediate **5** as reference structure at 0.0 kcal/mol. Visual inspection of Figure 2c clearly indicates that conversion of [(≡SiO-)W(=carbene)$(Me)_2$(H)] **5** to [(≡SiO-)W(=carbene)(cycloalkyl)$(Me)_2$] species **1**, **9** and **9a** is an exergonic process; conversion to **9b** is an endergonic process. In addition, the stability of [(≡SiO-)W(=carbene)(cycloalkyl)$(Me)_2$] species, **9a** > **9** ≈ **1** > **9b**, is in agreement with the product formation observed under non-confined conditions (**A0**) or with supports having large pore sizes (**A1**). Further, results underline the relevance of ring strain in determining the product distribution (Figure S4, ESI†).[38] Kinetic selectivity between the different pathways is determined at the level of the transition state corresponding to ring-opening of the metallacycle. According to calculations, the cC_7-pathway, with a ring opening transition state at 20.5 kcal/mol is favored, followed by the cC_8- and cC_{16}- pathways, with a ROM transition state at 21.6 and 23.8 kcal/mol, respectively. The corresponding transition state for the cC_9-pathway, at 30.7 kcal/mol, is clearly of higher energy, which might explain why the formation of cC_9 was experimentally not observed. Intermediate **6b** rather interacts with another cC_8-molecule (e.g. leading to cC_{17} without further DBM) rather than forming cC_9 by RCM. Comparing the cC_7- and the cC_{16}-pathway, the maximum energy barriers differ by around 3 kcal/mol. Finally, the rather low rate determining barrier of 21.6 kcal/mol on the cC_8-pathway might permit non-productive metathesis leading to the back formation of cC_8, as evidenced in Ru-catalyzed olefin metathesis metathesis.[39-40] Hence, the TON determined from the amount of detected (ring contracted and macrocyclic) products seems lower, because it does not include degenerate metathesis.

To rationalize the different product distributions obtained with **A1**, **A2** and **A3**, we focused on describing the main intermediates on the cC_{16}- and cC_7-pathways, namely **7** and **7a**, which are representative for each pathway. To demonstrate that the obtained selectivity originates from a confinement effect, replica exchange Monte Carlo simulations[41-42] were performed to calculate average effective volume (V_{eff}) and Sterimol shape parameters (L, B_1 and B_5, ESI†)[17-18] of both intermediate.

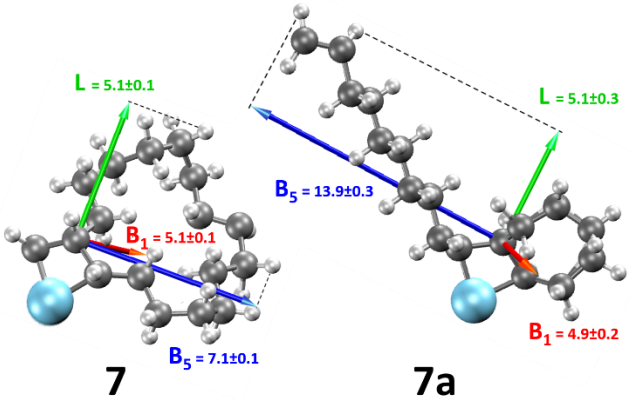

Figure 3. Representation of the Sterimol shape parameters (L, B_1 and B_5) of intermediates **7** and **7a**. L, B_1 and B_5 values for both intermediates are stated in Å near the respective axes.

The effective volumes of **7** (V_{eff}: 1530 ± 10 Å^3) and **7a** (V_{eff}: 1730 ± 10 Å^3) indicate that the formation of **7a** requires more space than the formation of **7** (Table S4, ESI†) which already supports the hypothesis that confinement effects determine the product distribution. It has been already reported that immobilization of either organic moieties (hybrid materials)[43,44] or organometallic complexes (SOMC)[45] inside mesoporous material (as SBA15 and MCM41) induces a considerable reduction of the pore size determined by N_2 sorption combined with low angle powder X-Ray diffraction. Thus, one has to consider that the actual pore size of **A1**, **A2** and **A3** decreases during cyclooctane metathesis, as the pre-catalyst **A** [(≡SiO-)WMe_5] reacts with cC_8 to form intermediates as **7**, **7a** and **5**. Considering intermediate **5**, the confinement effect might enhance the formation

of the *cis*-isomer of **5** facilitating the formation of the dimer cC_{16}. To have a more compelling evidence, we analyzed the Sterimol shape parameters L, B_1 and B_5 (Figure 3, ESI†). As expected, the L and B_1 parameters are quite similar in **7** and **7a**, namely L (**7**: 5.1±0.1 Å and **7a**: 5.1±0.3 Å) and B_1 (**7**: 5.1±0.3 Å and **7a**: 4.9±0.2 Å). Differently, the B_5 parameter, measuring the maximum size of the system perpendicular to the L parameter, shows pronounced differences (Figure 3). Specifically, the B_5 of **7** (bearing a cyclohexadecyl-residue) measures 7.1±0.1 Å and indicates that this intermediate is more compact and conformationally rigid than **7a** (bearing a flexible *n*-decenylidene-chain) having a B_5 of 13.9±0.3 Å. The clearly larger value of the B_5 parameter in **7a** relative to **7** strongly supports the hypothesis that the product distribution is determined by confinement effects. Hence, the formation of intermediate **7a** becomes more challenging under confined conditions, because the alkyl-chain might interact with its environment, whereas under non-confined conditions it can move freely. DBM cannot be fully avoided working with the multifunctional catalyst [(≡SiO-)W=CH_2(Me)$_2$H] **D**, which can perform ROM-RCM and (de-)hydrogenation at the same time due to (i) the presence of [W]-species on the external surface and (ii) alternative pathways, *e.g.* through intermediate **G**.

In conclusion, we found that confinement effects can modulate the product selectivity in cC_8 metathesis when [(≡SiO-)WMe_5] **A** is immobilized inside the mesopores of MCM41. In a confined environment, the formation of ring contracted products (as cC_7) is minimized because the key intermediates along the cC_7-pathway bear flexible alkyl chains which might interact with the environment. Contrary, intermediates along the cC_{16}-pathway are more compact and hence less affected under confined conditions. These results indicate a strategy for designing more selective catalysts by confining bulky transition states and intermediates of unfavourable side products. Works for improving the TON are currently ongoing in our laboratories using bimetallic catalysts.[46-47]

ASSOCIATED CONTENT

Supporting Information. Experimental and computation details. The Supporting Information is available free of charge on the ACS Publications website.

AUTHOR INFORMATION

Corresponding Author

jeanmarie.basset@kaust.edu.sa
luigi.cavallo@kaust.edu.sa
anissa.bendjeriousedjerari@kaust.edu.sa

ACKNOWLEDGMENT

The research reported in this publication was supported by funding from the King Abdullah University of Science and Technology (KAUST). The authors are grateful to the KAUST Supercomputing Laboratory (KSL) for the resources provided.

REFERENCES

(1) Derouane, E. G. *J. Catal.* **1986**, *100*, 541-544.
(2) Goettmann, F.; Sanchez, C. *J. Mater. Chem.* **2007**, *17*, 24-30.
(3) Polarz, S.; Kuschel, A., *Chem. Eur. J.* **2008**, *14*, 9816-9829.
(4) Thomas, J. M.; Raja, R. *Acc. Chem. Res.* **2008**, *41*, 708-720.
(5) Li, C. *Catal. Rev.-Sci. Eng.* **2004**, *46*, 419-492.
(6) Janda, A.; Vlaisavljevich, B.; Lin, L. C.; Smit, B.; Bell, A. T. *J. Am. Chem. Soc.* **2016**, *138*, 4739-56.
(7) Kenmogne, R.; Finiels, A.; Cammarano, C.; Hulea, V.; Fajula, F. *J. Catal.* **2015**, *329*, 348-354.
(8) Corma, A. In *Zeolite microporous solids: synthesis, structure, and reactivity; Derouane, E. G.; Lemos, F.; Naccache, C.; Ribeiro, F. R., eds.;* Springer Science & Business Media **2012**; pp 352, 1-611.
(9) Lesthaeghe, D.; Van Speybroeck, V.; Waroquier, M., *Phys. Chem. Chem. Phys.* **2009**, *11*, 5222-5226.
(10) Bru, M.; Dehn, R.; Teles, J. H.; Deuerlein, S.; Danz, M.; Mueller, I. B.; Limbach, M. *Chem. Eur. J.* **2013**, 19, 11661-11671.
(11) Basset, J.-M.; Callens, E.; Riache, N. In Handbook of Metathesis, Grubbs, R. H.; Wenzel, A. G. O'Leary, D. J. Khosravi, E., Eds.; *Wiley-VCH Verlag GmbH & Co. KGaA*, **2015**, pp 33-70.
(12) Basset, J. M.; Coperet, C.; Soulivong, D.; Taoufik, M.; Cazat, J. T., *Acc. Chem. Res.* **2010**, *43*, 323-334.
(13) Ahuja, R.; Kundu, S., Goldman, A. S.; Brookhart, M.; Vicente, B. C.; Scott, S. L. *Chem. Comm.* **2008**, 253-255.
(14) Pelletier, J. D. A.; Basset, J. M. *Acc. Chem. Res.* **2016**, 664-677.
(15) Huang, Z.; Rolfe, E.; Carson, E. C.; Brookhart, M.; Goldman, A. S.; El-Khalafy, S. H.; MacArthur, A. H. R. *Adv. Synth. Catal.* **2010**, *352*, 125-135.
(16) Riache, N.; Callens, E.; Samantaray, M. K.; Kharbatia, N. M.; Atiqullah, M.; Basset, J. M. *Chem. Eur. J.* **2014**, *20*, 15089-15094.
(17) Samantaray, M. K.; Dey, R.; Abou-Hamad, E.; Hamieh, A.; Basset, J.-M. *Chem. Eur. J.* **2015**, 21, 6100-6106;
(18) Verloop, A.; Hoogenstraaten, W.; Tipker J. In *Development and Application of New Steric Substituent Parameters in Drug Design*; Academic Press: New York, **1976**; Vol III, 165-207.
(19) Verloop, A. In The Sterimol Approach to Drug Design, Dekker, M., Eds., New York **1987**.
(20) Coperet, C.; Chabanas, M.; Saint-Arroman, R. P.; Basset, J. M. *Angew. Chem. Int. Ed.* **2003**, *42*, 156-181.
(21) Basset, J.-M.; Psaro, R.; Roberto, D.; Ugo, R., *Modern surface organometallic chemistry.* John Wiley & Sons, **2009**.
(22) Samantaray, M. K.; Callens, E.; Abou-Hamad, E.; Rossini, A. J.; Widdifield, C. M.; Dey, R.; Emsley, L.; Basset, J. M. *J. Am. Chem. Soc.* **2014,** *136*, 1054-1061.
(23) Pump, E.; Viger-Gravel, J.; Abou-Hamad, e.; Samantaray, M.K.; Hamzaoui, .; Gurinov, A.; Anjum, D. H.; Gajan, D.; Lesage, A.; Bendjeriou-Sedjerari, A.; Emsley, L.; Basset, J.-M. *Chem. Sci.* **2017**, *8*, 284-290.
(24) Le Roux, E.; Taoufik, M.; Chabanas, M.; Alcor, D.; Baudouin, A.; Coperet, C.; Thivolle-Cazat, J.; Basset, J. M.; Lesage, A.; Hediger, S.; Emsley, L. *Organometallics* **2005**, *24*, 4274-4279.
(25) Le Roux, E.; Taoufik, M.; Copéret, C.; de Mallmann, A.; Thivolle-Cazat, J.; Basset, J.-M.; Maunders, B. M.; Sunley, G. J., *Angew. Chem. Int. Ed.* **2005**, *44*, 6755-6758.
(26) Le Roux, E.; Taoufik, M.; Baudouin, A.; Coperet, C.; Thivolle-Cazat, J.; Basset, J. M.; Maunders, B. M.; Sunley, G. J., *Adv. Synth. Catal.* **2007**, *349*, 231-237.
(27) Zhao, D. Y.; Huo, Q. S.; Feng, J. L.; Chmelka, B. F.; Stucky, G. D. *J. Am. Chem. Soc.* **2014**, *136*, 10546-10546.
(28) Berenguer-Murcia, A.; Garcia-Martinez, J.; Cazorla-Amoros, D.; Martinez-Alonso, A.; Tascon, J. M. D.; Linares-Solano, A. In Studies in Surface Science and Catalysis 144; Rodriguez-Reinoso, F., McEnaney, B., Rouquerol, J., Unger, K., Eds.; Elsevier Science: Amsterdam, **2002**; pp 83-90.
(29) Choi, S. W.; Bae, H. K. *J. Civil Eng.* **2014**, *18*, 1977-1983.
(30) Cu, G.; Ong, P. P.; Chu, C. *J. Phys. Chem. Solids* **1999**, *60*, 943-947.

(31) Soignier, S.; Taoufik, M.; Le Roux, E.; Saggio, G.; Dablemont, C.; Baudouin, A.; Lefebvre, F.; de Mallmann, A.; Thivolle-Cazat, J.; Basset, J. M.; Sunley, G.; Maunders, B. M. *Organometallics* **2006**, *25*, 1569-1577.
(32) Callens, E.; Riache, N.; Talbi, K.; Basset, J. M., *Chem. Comm.* **2015**, *51*, 15300-15303.
(33) Bagwe, R. P.; Hilliard, L. R.; Tan, W. *Langmuir* **2006**, *22*, 4357-4362.
(34) Maity, N.; Barman, S.; Callens, E.; Samantaray, M. K.; Abou-Hamad, E.; Minenkov, Y.; D'Elia, V.; Hoffman, A. S.; Widdifield, C. M.; Cavallo, L.; Gates, B. C.; Basset, J.-M. *Chem. Sci.* **2016**, *7*, 1558-1568.
(35) Callens, E.; Abou-Hamad, E.; Riache, N.; Basset, J. M., *Chem. Comm.* **2014**, *50*, 3982-3985.
(36) Schrock, R. R. In *Alkene Metathesis in Organic Synthesis*; *Fuerstner, A., ed*., Springer, **1998**; pp 1-36.
(37) Leconte, M.; Basset, J., J. Am. Chem. Soc. **1979**, *101*, 7296-7302.
(38) Anslyn, E. V.; Dougherty, D. A. In *Modern Physical Organic Chemistry,* University Science Books, Sausalito, **2006**, pp. 65-144.
(39) Stewart, I. C.; Keitz, B. K.; Kuhn, K. M.; Thomas, R. M.; Grubbs, R. H. *J. Am. Chem. Soc.* **2010**, *132*, 8534-8535.
(40).Wenzel, A. G. In *Handbook of Metathesis, 2nd ed., Grubbs, R.H., Wenzel, A. G.; O'Leary, D. J.; Khosravi, E., eds*.; Wiley-VCH Verlag GmbH & Co. KGaA: **2015**, Vol. 3, pp 253-272.
(41) Sugita, Y.; Okamoto, Y., *Chem. Phys. Lett.* **1999**, *314*, 141-151.
(42) Zhou, R. H.; Berne, B. J., *Proc. Natl. Acad. Sci. U. S. A.* **2002**, *99*, 12777-12782.
(43) Anwander, R.; Nagl, I.; Widenmeyer, M.; Engelhardt, G.; Groeger, O.; Palm, C.; Röser, T., *J. Phys. Chem. B* **2000**, *104*, 3532-3544.
(44). Margelefsky, E. L.; Bendjériou, A.; Zeidan, R. K.; Dufaud, V.; Davis, M. E. *J. Am. Chem. Soc.* **2008**, *130*, 13442-13449.
(45) Bendjeriou-Sedjerari, A.; Azzi, J. M.; Abou-Hamad, E.; Anjum, D. H.; Pasha, F. A.; Huang, K. W.; Emsley, L.; Basset, J. M., *J. Am. Chem. Soc.* **2013**, *135*, 17943-17951.
(46) Samantaray, M. K.; Dey, R.; Kavitake, S.; Abou-Hamad, E.; Bendjeriou-Sedjerari, A.; Hamieh, A.; Basset, J.-M. *J. Am. Chem. Soc.* **2016**, *138*, 8595-8602.
(47) Samantaray, M. K.; Kavitake, S.; Morlanés, N.; Abou-Hamad, E.; Hamieh, A.; Dey, R.; Basset, J.-M., *J. Am. Chem. Soc.* **2017**, *139*, 3522-3527.

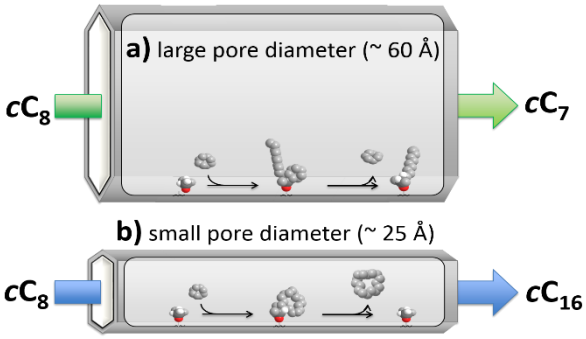
a) large pore diameter (~ 60 Å)
cC8
cC7
b) small pore diameter (~ 25 Å)
cC8
cC16